Changes of the electronic structure of Cu-Pt due to order-disorder transitions

J. Banhart
Institut für Physikalische Chemie, Universität München, Sophienstrasse 11, 8000 München 2, Federal Republic of Germany

R. Kuentzler
Institut de Physique et Chimie des Materiaux de Strasbourg, 3, rue de l'Université, 67084 Strasbourg, France

W. Pfeiler
Institut für Festkörperphysik, Universität Wien, Strudlhofgasse 4, 1090 Wien, Austria

T. Christ
Institut für Physikalische Chemie, Universität München, Sophienstrasse 11, 8000 München 2, Federal Republic of Germany

P. Weinberger
Institut für Technische Elektrochemie, Technische Universität Wien, Getreidemarkt 9, 1060 Wien, Austria

J. Voitländer
Institut für Physikalische Chemie, Universität München, Sophienstrasse 11, 8000 München 2, Federal Republic of Germany
(Received 24 May 1991)

The changes of the electronic structure of Cu-Pt undergoing an order-disorder transition have been investigated by measuring the linear coefficient of the low-temperature specific heat γ and the nuclear spin-lattice relaxation time T_1 of ^{195}Pt. The observed changes of the values of γ and T_1 can be interpreted by comparing them with theoretical values based on relativistic Korringa-Kohn-Rostoker coherent-potential-approximation and embedded-cluster-method calculations. The influence of short-range order on the electronic structure has also been investigated.

I. INTRODUCTION

Order phenomena in binary alloys and their electronic structure are closely related to each other. The electronic energy may be order dependent and therefore causes the formation of ordered or disordered structures. Numerous theories have been developed to predict the occurrence of order from the knowledge of the electronic structure.[1] This paper however deals with the reverse problem: How does a given degree of order influence certain electronic properties? Experiments and theoretical calculations have been carried out in order to answer this question. We concentrated on observables which depend on properties of electrons on the Fermi surface, namely, the linear coefficient of the low-temperature specific heat γ and the nuclear spin-lattice relaxation time T_1. Both quantities can be measured. The order dependence of the specific heat of alloys has been measured for some alloy systems (e.g., Cu-Pd,[2] Cu-Pt[3,4]), whereas that of T_1 has not yet been investigated as far as we know.

The density of states (DOS) and the spin-lattice relaxation time can be calculated from the one-particle Green's function. In this work we confine ourselves to the *change* of the observables mentioned above under a transition between the disordered and the long-range or short-range ordered state. For the calculations we choose a description for the electronic structure of both the ordered and the disordered states based on the same numerical procedure, namely, the relativistic Korringa-Kohn-Rostoker coherent- potential-approximation (KKR-CPA) and the relativistic embedded-cluster-method (ECM)-CPA.

The alloy system Cu-Pt is especially suitable to be studied.

(i) The phase diagram of Cu-Pt (Ref. 5) is comparatively simple. Occurrence of short-range order (SRO) and long-range order (LRO) can easily be observed and the kinetics of SRO and LRO formation were investigated by resistivity measurements.[6,7] The order-disorder transition of $Cu_{50}Pt_{50}$ is of first order[8] and does hardly change the lattice constant[9] therefore facilitating the calculations.

(ii) The NMR transitions of ^{195}Pt in Cu-Pt are not disturbed by quadrupolar interactions and are sufficiently intense therefore allowing a precise determination of the spin-lattice relaxation time.

(iii) This alloy system was already investigated theoretically by us.[10–13]

(iv) The energy dependent DOS has a large slope at the Fermi energy at least for the Pt component. Therefore order in this alloy system should strongly effect γ and T_1.

We first describe experimental details and the theoretical procedures and then discuss the results for the different types of ordered structures.

II. EXPERIMENTAL

A. Sample preparation

Alloy samples of various compositions were prepared by Degussa (Hanau) by melting together appropriate amounts of Pt (99.99%) and Cu (99.999%). The alloy ingots were cut into small pieces and cold rolled step by step to foils of 50 μm thickness. Between the steps the samples were annealed in a purified argon atmosphere and then quenched into water of 20 °C . This quenching procedure is important in order to prevent the alloys from order hardening.

The cold-rolled alloy samples were assumed to be in a highly disordered state (see, e.g., Ref. 9). The alloy $Cu_{50}Pt_{50}$ was thermally treated to allow ordering into the $L1_1$ structure (CuPt). The temperature and duration of the thermal annealing treatment to achieve a long-range order equilibrium were determined from the relaxation behavior as obtained by resistivity measurement.[6,7,14] The annealing steps used were 850 °C: 1 h, 750 °C: 1 h, 700 °C: 2 h, 600 °C: 8 h, 500 °C: 18 h, 450 °C: 20 h. By resistivity measurements it has been proved that these annealing steps are sufficient for the alloy to reach equilibrium. On the one hand it is unnecessary to hold the temperature at 750 °C for several days as some authors have done (e.g., Refs. 15 and 16) because the relaxation time is very short at this temperature.[6] On the other hand the atomic mobility is minute below 450 °C and therefore no annealing was undertaken below this temperature.

The resistivity measurements suggested that it is possible to prepare states of pure short-range order in some Cu-Pt alloys even below the transition temperature to long-range order by making use of the different relaxation times of the various kinds of order. We prepared three different states of short-range order in $Cu_{65}Pt_{35}$ by means of the following heat treatment: The cold-rolled alloy samples were first exposed to a homogenizing pretreatment consisting of a slow heating up from room temperature to 850 °C and, after holding this temperature for 2 h, a slow cooling down to room temperature. Then the alloy was heated up to 850 °C again and quenched in water. To allow the development of short-range order the samples were annealed at 700 °C for 20 min and then quenched. One third of the samples was removed for measurement (→ sample 1). The rest was annealed a second time at 550 °C for 30 min and then quenched. One half of the samples was removed (→ sample 2) the remaining material annealed at 400 °C for 200 min and then quenched (→ sample 3). According to the results of the resistivity measurements on $Cu_{65}Pt_{35}$ (Refs. 6 and 7) samples 1, 2, and 3 were then in an equilibrium state of SRO corresponding to temperatures 700, 550, and 400 °C .

B. Specific heat measurements

The specific heat measurements were performed by means of a quasi-adiabatic method between 1.5 and 8 K. A newly developed apparatus used for the experiments operates automatically and has a temperature regulation based on a Cryocal germanium resistor.

Usually the specific heat of a metal or alloy obeys the law $C(T) = \gamma T + \beta T^3$, where the first term stands for the electronic contribution and the second for the lattice contribution. The density of states at the Fermi energy $n(E_F)$ can be deduced from γ and the Debye temperature Θ_D from β. In fact enhancement by electron-phonon ($\lambda_{e\text{-}p}$) coupling and spin fluctuations (λ_{SF}) can increase the bare DOS, so that γ is given by

$$\gamma = \tfrac{1}{3}\pi^2 k_B^2 \,(1 + \lambda_{e\text{-}p} + \lambda_{SF} + \cdots)\, n(E_F) \,. \qquad (1)$$

The accuracy of the raw data, plotted as C/T versus T^2 (see Fig. 1) is better than 1% for our samples. The excellent linearity of this plot down to 2 K yields an accuracy of about 1% for γ and 3% for Θ_D. The slight deviation from linearity below 2 K for the disordered sample is discussed in Sec. IV A.

C. NMR measurements

A Bruker pulsed NMR-spectrometer (SXP) was used for measuring the spin-lattice relaxation time of ^{195}Pt in Cu-Pt alloys. An Oxford Cryomagnet was operated at 7 T corresponding to a resonance frequency of about 63.5 MHz. The steady-flow cryostat allowed cooling down to 3.9 K. The temperature of the alloy was measured by a carbon glass resistor mounted very close to the sample limiting the inaccuracy of the temperature measurement to less than 3%. Fifteen $\pi/2$ (20 μs) saturation pulses were applied in order to destroy the longitudinal magnetization in the sample. After a delay time τ two $\pi/2$ pulses transferred the recovering magnetization into a spin echo, the intensity of which was determined by integrating the echo. The intensity was assumed to be proportional to the longitudinal magnetization $M_z(\tau)$. The relaxation time T_1 was determined by numerical analysis of the approximately 40–50 points corresponding to an appropriate choice of delay times τ. A model function of the form

$$M_z(\tau) = M_0 + (M_\infty - M_0)\,(1 - e^{-\tau/T_1}) \qquad (2)$$

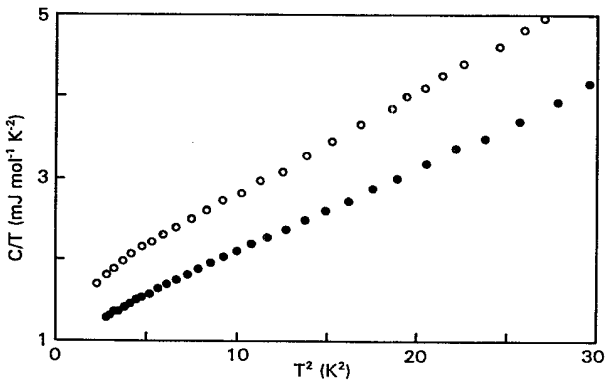

FIG. 1. C/T vs T^2 plot for disordered $Cu_{50}Pt_{50}$ (open circles) and ordered Cu-Pt (solid circles).

was fitted to the experimental data by least-squares approximation in order to determine the relaxation time T_1. M_0 is the rest magnetization not removed by the saturation pulses, M_∞ the equilibrium magnetization. The statistical error for T_1 was between 2 and 10 % depending on the intensity of the signal.

III. THEORETICAL APPROACH

A. Disordered state

Disorder is treated in the framework of the coherent potential approximation (CPA), namely, the relativistic KKR version of the CPA. The relativistic CPA equations[17] were solved for an angular momentum up to $l_{max} = 2$. The Brillouin-zone integration of the KKR matrix was carried out using 21 special directions[18] and between 30 and 900 k points in each direction. For the iterative solution of the CPA equations an improved iteration scheme for the KKR-CPA was used.[19] The Fermi energy was determined by use of Lloyd's formula for the integrated density of states.[17] All calculations were based on site potentials according to the Mattheiss description and on experimental lattice constants.[9] The CPA yields scattering path operators closely related to one-particle Green's functions $G^\alpha(E)$ corresponding to a real impurity of type α embedded in the averaged CPA medium. From these Green's functions the density of states $n^\alpha(E)$ (Refs. 17 and 20) and the nuclear spin-lattice relaxation rate $(T_1T)^{-1}$ (Ref. 21) can be calculated:

$$n^\alpha(E) = -\frac{1}{\pi}\mathrm{Im}\,\mathrm{Tr}\,[G^\alpha(E)] = \sum_\kappa n^\alpha_\kappa(E)\ , \tag{3}$$

$$(T_1T)^{-1}_\alpha = 4\pi k_B\hbar\left(\gamma^\alpha_N\frac{e}{2}\right)^2\left(\sum_\kappa\frac{2j+1}{6j(j+1)}\left[n^\alpha_\kappa(E_F)\bar{R}^\alpha_{\kappa,\kappa}(E_F)\right]^2+\sum_{\kappa>0}\frac{1}{3(j+1)}n^\alpha_\kappa(E_F)n^\alpha_{-\kappa-1}\left[\bar{R}^\alpha_{\kappa,-\kappa-1}(E_F)\right]^2\right)\ . \tag{4}$$

$\bar{R}$ are normalized radial matrix elements, κ and j are the usual angular momentum quantum numbers, γ^α_N is the gyromagnetic ratio of the nucleus of the atom of type α, and T is the temperature. $(T_1T)^{-1}$, the relaxation *rate*, is the quantity which enters the theoretical calculations, whereas T_1, the relaxation *time*, or T_1T are the quantities occurring in experiments. In this paper T_1T is used where experimental values are discussed. $(T_1T)^{-1}$ is used for theoretical discussions. Note also that in this paper all values for the DOS are taken at the Fermi energy.

B. Short-range order

Because of the single-site character of the averaging the CPA cannot account for the case of local order. An adequate theory requires a more complex averaging scheme. There is no alloy theory in existence yet which treats SRO on the same level of self-consistency as the CPA does for the case of disorder. Therefore a number of non-self-consistent theories have been proposed. The embedded cluster method (ECM) based on the CPA (Ref. 22) is one of these and has been proved to give a good description of SRO. It treats clusters of real atoms embedded in the single-site averaged CPA medium and yields scattering-path operators and Green's functions for clusters of definite configurations. For details of the calculation see Ref. 13. Several aspects of the application of the ECM to the system Cu-Pt have been discussed extensively in earlier papers.[10,11]

C. Long-range order

Alloys with long-range order have translational symmetry and therefore the standard band-structure methods can be applied [e.g., the Linear-Muffin-Tin-Orbital (LMTO) method]. However, for the purpose of this work, where physical observables of alloys in the ordered and disordered states were to be compared, the use of such methods did not appear to be suitable. As the numerical treatment of the band-structure problem requires other numerical methods than the realization of the CPA the sources of numerical errors of both methods are quite different. For example, the Fermi energy in the KKR-CPA is determined using an explicit formula for the integrated DOS whereas in the LMTO the peaky differential DOS has to be integrated numerically. Changing the numerical parameters of the LMTO calculation one could produce values for the DOS at the Fermi energy varying over a considerable range making predictions about the (sometimes tiny) order effect on the density of states (and the spin-lattice relaxation time) rather speculative. We therefore tried to treat the LRO on the same footing as the SRO, namely, on the base of the CPA. The idea is to approximate the global LRO structure locally by considering clusters occupied with atoms in the same arrangement as in the long-range ordered structure (see Fig. 2). For CuPt the sites of two or four shell clusters surrounding a central atom are occupied by either Cu or Pt in a manner that all atoms belonging to a particular (111) plane are all of the same type. The local DOS at the center of such an "ordered" cluster of a small number of shells can then be calculated and compared to the CPA-DOS. So the change of the electronic structure undergoing an order-disorder transition can be determined. This approximation works well for CuPt because of the following facts.

(i) It had been observed that the influence of shells more distant from the center (i.e., beyond the second shell) on the DOS is very small.[13]. Therefore to get a good approximation it is sufficient to consider the first

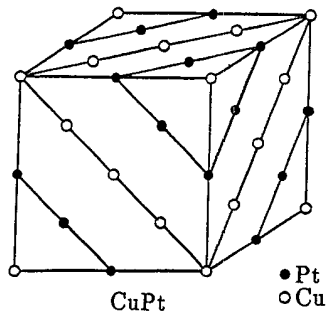

FIG. 2. The ordered CuPt structure ($L1_1$) (Ref. 9).

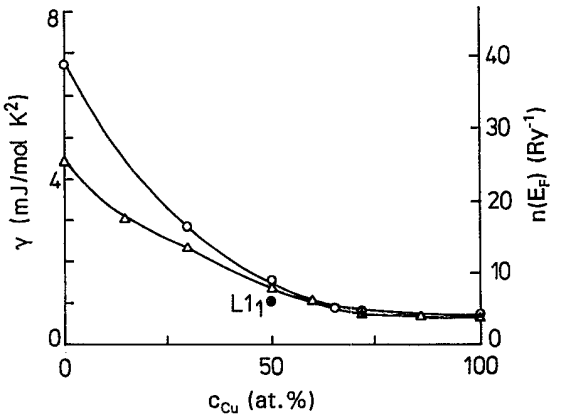

FIG. 3. Linear coefficient of the low-temperature specific heat γ and density of states at the Fermi energy $n(E_F)$ of CuPt. Open circles: measured γ [disordered alloys: this work, pure Pt: (Ref. 25), pure Cu: (Ref. 26)]. Solid circle: measured γ for the ordered alloy CuPt. Triangles: calculated $n(E_F)$ [disordered alloys: this work, pure Pt: (Ref. 27), pure Cu: (Ref. 28)].

two or four shells.

(ii) The lattice constants of the ordered and disordered phases are similar. Furthermore ordering does hardly affect the spatial positions of the atomic sites in the crystal.[9]

(iii) The energy-dependent CPA-DOS and the corresponding DOS of the two-shell "ordered" cluster are similar. If the DOS $n(E)$ is integrated over the energy for both structures in order to obtain the integrated DOS and the Fermi energy, the Fermi energy level is found to be nearly identical for both cases. Therefore the use of the same Fermi energy for both the disordered and the ordered structure is justified.

For the calculation of the electronic structure of the long-range ordered state approximated in this way one merely has to calculate the scattering path operators (and from these the Green's functions) for two "ordered" clusters, one with a Cu atom and one with a Pt atom at the center.

IV. RESULTS AND DISCUSSION

A. Disordered state

The linear coefficient of the low-temperature specific heat γ and the spin-lattice relaxation time T_1 of ^{195}Pt were measured for four different compositions of disordered (cold rolled) Cu-Pt alloys (30, 50, 65, 71 at.% Cu) and compared with the corresponding calculated values based on the results of the KKR-CPA in order to check the agreement between experiment and theory.

1. Specific heat

In Fig. 3 the measured values for γ and the calculated densities of states at the Fermi energy $n(E_F)$ are shown. For the ordinate units of the DOS (1/Ry) and units of the specific heat coefficient [mJ/(mol K^2)] are used [with the relation $\gamma = \frac{1}{3}\pi^2 k_B^2 n(E_F)$]. Of course this formula neglects the enhancement of γ by electron-phonon coupling, spin fluctuations, etc. For Pt spin fluctuations contribute predominantly to the enhancement factor. So it is not surprising that the difference between $n(E_F)$ and γ grows as the Pt content increases. The experimental and theoretical results thus agree with each other quite well. All results are listed in Table I including the Debye temperatures Θ_D which were derived from the slopes of the temperature-dependent experimental specific heats in Fig. 1. The C/T versus T^2 curve for the disordered (cold-rolled) sample exhibits a small deviation from linearity below 2 K. This may possibly be an effect of positional disorder ("amorphization") caused by cold rolling. In spite of this effect our result for the disordered sample $Cu_{50}Pt_{50}$ [1.55 mJ/(mol K^2)] agrees well with the result of Ref. 15 [1.59 mJ/(mol K^2)].

2. Spin-lattice relaxation time

In Fig. 4 the experimentally determined values for T_1T are compared with values measured by other authors[23]

TABLE I. Results of the measurements of the specific heat (linear coefficient γ and Debye temperature Θ_D) and the spin-lattice relaxation time T_1T.

at.% Cu	Structure	γ [mJ/(mol K^2)]	Θ_D (K)	T_1T (ms K)
30	Disordered	2.92	254	71
50	Disordered	1.55	250	82, 90
	Ordered	1.04	265	132
65	Disordered	0.96	253	85
	SRO 700 °C			84
	SRO 550 °C			86
	SRO 400 °C	1.04	264	82
71	Disordered	0.82	270	87

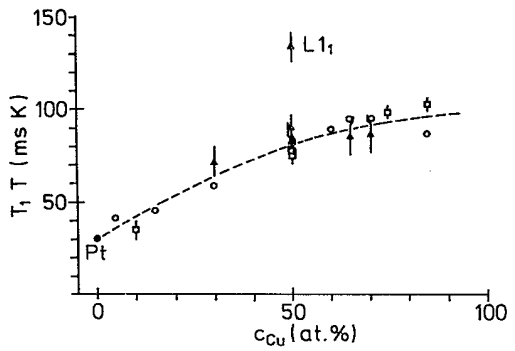

FIG. 4. T_1T of ^{195}Pt in Cu-Pt. All values except the one marked ($L1_1$) are for the disordered (cold-rolled) state. Triangles: experimental values (this work): $T = 3.9$ K, B_0=6.95 T, $\nu\approx$63.5 MHz. Squares: experimental values (Ref. 23). Solid circle: experimental value for pure Pt (Ref. 29). Open circles: calculated values. Dashed line: general tendency.

and also with our theoretical values calculated from the KKR-CPA densities of states using Eq. (4). Apparently the experimental values for the Cu-Pt alloys indicate an increase of T_1T with increasing Cu content. The experimental values of this work agree with those of Itoh *et al.* The calculated values reflect the general tendency of the experimental results. It should be noted that the calculated values in this work differ slightly from those published earlier[10,11] due to a more precise determination of the Fermi energy in this work.

B. Long-range ordered state

1. Density of states

Figure 5 shows the DOS for the disordered and the ordered structures. The CPA-DOS for the disordered alloy is compared to the DOS of an ordered alloy calculated with the two-shell approximation to the ECM. The difference between the CPA- and the ECM-DOS is comparatively small. This is due to the fact that the transition from the disordered to the ordered state leaves the occupation numbers of the first shell around a specified atom unchanged. This means that the first shell around, for example, a Pt atom consists of 6 Cu and 6 Pt atoms in the disordered (on the average) and in the ordered (exactly) alloy. The effect of the disorder-order transition on the first shell can therefore be seen as merely a change in the positions of some Cu and Pt atoms within the shell in order to form the ordered pattern. The local DOS at the central Pt atom however depends mainly on the number of Cu and Pt atoms in the first shell which is 6:6 in both cases, not on their spatial position.[10] So the changes arise from the more distant second shell where the occupation numbers change from Cu:Pt=3:3 for the disordered state to 6:0 (0:6) for the ordered state with Pt (Cu) in the origin and are therefore less pronounced.

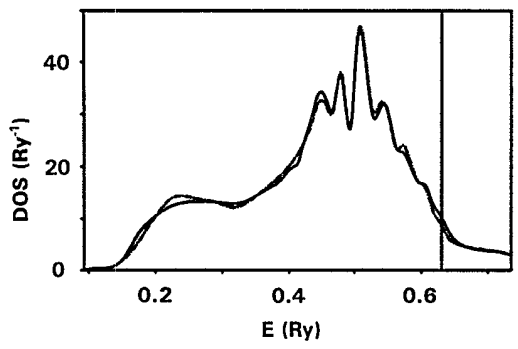

FIG. 5. Density of states of $Cu_{50}Pt_{50}$. Solid line: CPA-DOS, dash-dotted line: ECM-DOS for two shell ordered clusters. The Fermi energy is marked by a vertical line.

The main feature in the ECM-DOS in Fig. 5 is that there are less electrons near the Fermi energy than in the CPA-DOS. These electrons appear at lower energies around 0.4 and 0.23 Ry. The sum of all one-electron energies (which is of course not the binding energy) is therefore lower in the ordered structure.

2. Specific heat

The coefficient γ was measured for the ordered CuPt alloy. The result [1.04 mJ/(mol K^2)] is in an excellent agreement with values measured by other authors (1.02,[15] 1.040,[16] note that the first result has been corrected following the arguments given in the second reference). Thus ordering leads to a drastic decrease of γ by 35% (Fig. 6 left side). The calculated density of states

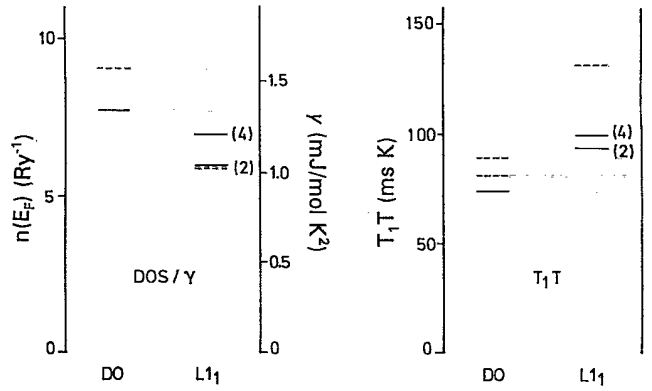

FIG. 6. Comparison of the measured and calculated quantities for the disordered (DO) and ordered ($L1_1$) states. Left part: measured specific heat coefficient γ (dashed lines) and corresponding calculated DOS (solid lines). DOS for the disordered state by the CPA, DOS for the ordered state by the 2- and 4-shell approximations to the ECM. Right part: measured T_1T (dashed lines, two results for DO) and calculated T_1T (solid lines). Values for the disordered state by the CPA, for the ordered state by the 2- and 4-shell approximations to the ECM. All displayed values are contained in Tables I, II, and III.

TABLE II. Angular momentum resolved DOS of disordered $Cu_{50}Pt_{50}$ and ordered CuPt calculated with the CPA or the ECM-CPA, respectively. Units: 1/Ry.

Structure	Atom	$s_{1/2}$	$p_{1/2}$	$p_{3/2}$	$d_{3/2}$	$d_{5/2}$	Sum	Total
Disordered	Cu	0.29	0.16	0.39	1.19	2.11	4.14	7.74
	Pt	0.26	0.14	0.25	2.26	8.42	11.34	
Ordered	Cu	0.29	0.16	0.38	1.08	1.91	3.82	6.21
(2 shells)	Pt	0.26	0.15	0.25	1.61	6.32	8.59	
Ordered	Cu	0.24	0.17	0.44	1.11	1.98	3.93	6.99
(4 shells)	Pt	0.28	0.13	0.23	1.90	7.52	10.06	

shows the same behavior. Applying a two-shell cluster approximation the DOS drops by about 20% from the disordered state (CPA) to the ordered state, however by only 10% applying a four-shell cluster approximation. A calculation with six shells (not yet feasible) would probably lead to a decrease between 10 and 20 % because the sixth shell is occupied by Pt atoms only. This means that the cluster approximation of LRO is able to explain the general behavior of the DOS. More details of the change of the DOS associated with the order-disorder transition can be seen from the angular momentum resolved DOS in Table II. Apparently the s and p contributions to the DOS are nearly independent of the state of order. Merely the d components are strongly order dependent. The main change is due to the local DOS of Pt. As already mentioned the number of Cu atoms in the first shell around a Pt atom does on an average not change by ordering but the number of Cu atoms in the second shell increases from three to six, causing a strong decrease of the DOS. One could think that the inclusion of a higher number of shells in this kind of approximation would lead to a convergent sequence of densities of states, but probably this is not the case owing to the non-self-consistency of the ECM-CPA.

In the discussion so far we assumed that the contributions to γ due to nonelectronic mechanisms [represented by the various λ in Eq. (1)] are the same in the ordered and the disordered states ($\lambda_{tot} \approx 0.15$). This does not have to be true. If λ changed under an order-disorder transition this would give rise to an extra increase or decrease to γ. As our calculations are approximations we cannot estimate this effect here.

3. *Spin-lattice relaxation time*

Ordering causes the measured T_1T of ^{195}Pt to increase drastically (Figs. 4 and 6). The increase of T_1T is related to the decrease of the DOS at the Fermi energy which causes a weaker coupling of the nuclear spins to the electrons on the Fermi surface and therefore leads to a slower relaxation due to the interaction with the lattice. However, the spin-lattice relaxation time gives different information compared with the DOS or γ. Firstly the spin-lattice relaxation time is a local probe because it measures only the Pt contributions to the DOS and secondly the various angular momentum contributions are weighted in a different manner [compare the right-hand side of Eq. (3) with Eq. (4)]. The most important difference between DOS and T_1T is the large s-like contribution to T_1T due to the hyperfine interaction betweeen the electrons and the Pt nuclei, having no counterpart in the DOS.

The change of the spin-lattice relaxation time is more pronounced (more than 50%) than that of the DOS. In Fig. 6 the experimental and theoretical values for T_1T are compared. The two-shell approximation leads to an increase of T_1T of 30%, the four-shell approximation to an increase of 36%. Again the theoretical approach yields a correct qualitative description of the behavior of a physical observable. Table III lists the calculated angular momentum resolved components of $(T_1T)^{-1}$. As in the case of the DOS the main contribution to the order dependence is due to the d components of $(T_1T)^{-1}$. Contrary to the case of the DOS the result of the four-shell

TABLE III. Relaxation rates $(T_1T)^{-1}$ of ^{195}Pt in disordered $Cu_{50}Pt_{50}$ and ordered CuPt calculated with the CPA or the ECM-CPA, respectively. Columns 2–6: 5 diagonal components (l_j, l_j), columns 7 and 8: $(p_{1/2}, p_{3/2})$ and $(d_{3/2}, d_{5/2})$ components (abbreviated as p-p and d-d). Units of relaxation rates $(Ks)^{-1}$.

Structure	$s_{1/2}$	$p_{1/2}$	$p_{3/2}$	$d_{3/2}$	$d_{5/2}$	p-p	d-d	Sum
Disordered	5.24	0.17	0.03	2.61	5.46	0.002	0.07	13.57
Ordered (2 shells)	5.28	0.17	0.03	1.45	3.42	0.004	0.08	10.44
Ordered (4 shells)	6.10	0.14	0.02	0.93	2.75	0.003	0.07	10.02

approximation for $(T_1T)^{-1}$ is closer to the true (experimental) value than that of the two-shell approximation. This is due to the large-s contributions from the fourth shell not present in the DOS. Looking at the values of the s- and p-contributions to $(T_1T)^{-1}$ in Table III it is apparent that the difference between the two- and the four-shell approximation is larger than that between the two-shell approximation and the CPA result. This again demonstrates that we are not dealing with a convergent sequence when the number of shells is increased.

4. Remark on the magnetic susceptibility

The magnetic susceptibility of $Cu_{50}Pt_{50}$ decreases from +1.8 to −3.8 cm^3/mol (Ref. 24) at the transition from the disordered to the ordered state. Although only part of the magnetic susceptibility is directly proportional to the density of states, the total susceptibility shows the same tendency as the DOS.

C. Short-range ordered state

1. Spin-lattice relaxation time

The spin-lattice relaxation time was measured for the alloy $Cu_{65}Pt_{35}$ in three different states of SRO. In Fig. 7 T_1T for the short-range ordered state is shown together with the result for the cold-rolled (disordered) state (corresponding to an "infinite" temperature). Apparently T_1T is nearly constant in the investigated temperature range. This is in accordance with the calculated SRO dependent T_1T. Figure 8 shows the calculated T_1T of ^{195}Pt in $Cu_{65}Pt_{35}$ depending on the short-range order parameter of the first and second shells α_1 and α_2 (for details of the calculation see Ref. 13). In Fig. 7 the abscissa is given in units of the temperature, in Fig. 8 in units of the SRO parameter α. We know that SRO (negative values of α) is destroyed by high temperatures and that $\alpha = 0$ for $T \to \infty$. $\alpha(T)$ is therefore a monotonously increasing function. The exact function is not known. Now, the calculated T_1T varies by only about 6% over the whole range of α in Fig. 8 $(1-1/\max\{c_A, c_B\} < \alpha < 0$; c_A, c_B are the concentrations of the components A and $B)$. The range of the experimentally prepared short-range ordered states

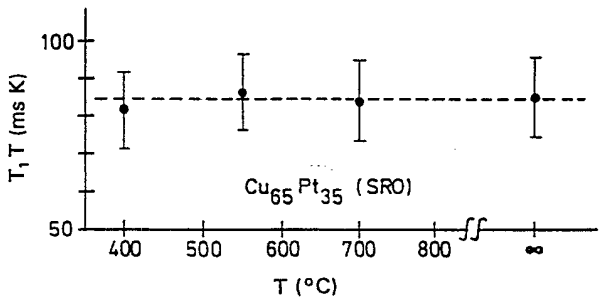

FIG. 7. T_1T of ^{195}Pt in $Cu_{65}Pt_{35}$ in equilibrium states of *SRO* belonging to the temperature T and in the cold-rolled (disordered) state belonging to temperature T=∞.

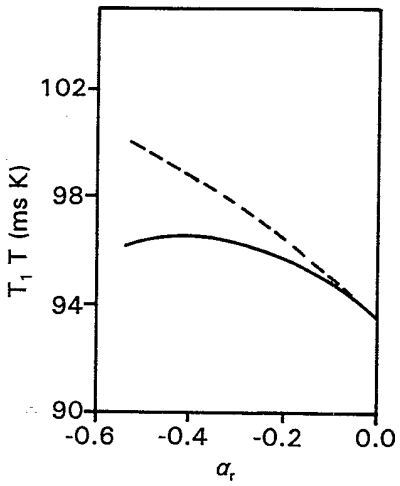

FIG. 8. Calculated values of T_1T of ^{195}Pt in $Cu_{65}Pt_{35}$ depending on the short-range order parameters. (– – –): α_1, (——): α_2.

only covers a fraction of this range because on the one hand due to the long relaxation times of short-range ordering at low temperatures one cannot achieve the maximum value of SRO and on the other hand even the "disordered" experimental probes have still some SRO. So the variation of T_1T over the whole temperature range would be less than 6% and T_1T is therefore constant in the limits of experimental accuracy.

2. Specific heat

A similar behavior as for T_1T is found for the linear coefficient of the specific heat. For $Cu_{65}Pt_{35}$ with short-range order corresponding to a temperature of 400 °C the value of γ is 1.04 mJ/(mol K^2), nearly the same as for the disordered sample [0.96 mJ/(mol K^2)]. The calculated SRO dependence of γ is also very small,[13] similar to the SRO dependence of T_1T shown in Fig. 8.

V. CONCLUSION

(i) Experiments and calculations indicate a strong influence of LRO on γ and T_1T, reflecting the close relation between order and electronic structure.

(ii) The ECM method is well suited for an approximate treatment of LRO.

(iii) In $Cu_{65}Pt_{35}$ no significant change of γ or T_1T is observed for the relatively small changes in the SRO parameters accessible to experiments.

ACKNOWLEDGMENTS

We would like to thank Degussa (Hanau) for supplying Cu-Pt alloy samples. This work was financially supported by the Österreichischer Fonds zur Förderung der wissenschaftlichen Forschung (Grant No. 5894), the Österreichische Forschungsgemeinschaft, and the Deutsche Forschungsgemeinschaft.

[1] A. Gonis, X.G. Zhang, A.J. Freeman, P. Turchi, G.M. Stocks, and D.M. Nicholson, Phys. Rev. B **36**, 4630 (1987).
[2] Y. Sato, J.M. Sivertsen, and L.E. Toth, Phys. Rev. B **1**, 1402 (1970).
[3] R. Kuentzler, Phys. Status Solidi B **58**, 519 (1973).
[4] R. Kuentzler, Inst. Phys. Conf. Ser. **55**, 397 (1980).
[5] M. Hansen and K. Anderko, *Constitution of Binary Alloys* (McGraw-Hill, New York, 1958).
[6] J. Banhart, W. Pfeiler, and J. Voitländer, Phys. Rev. B **37**, 6027 (1988).
[7] J. Banhart, W. Pfeiler, and J. Voitländer, in *Alloy Phase Stability*, Vol. 163 of *NATO Advanced Study Institute Series E*: Applied Physics, edited by G.M. Stocks and A. Gonis (Kluwer, Dordrecht, 1989), p. 131.
[8] R.S. Irani and R.W. Cahn, J. Mater. Sci. **8**, 1453 (1973).
[9] J.O. Linde, Ann. Phys. **30**, 151 (1937).
[10] J. Banhart, P. Weinberger, H. Ebert, and J. Voitländer, Solid State Commun. **65**, 693 (1988).
[11] J. Banhart, H. Ebert, P. Weinberger, and J. Voitländer, J. Appl. Phys. **63**, 4130 (1988).
[12] J. Banhart, P. Weinberger, and J. Voitländer, J. Phys. Condens. Matter **1**, 7013 (1989).
[13] J. Banhart, P. Weinberger, and J. Voitländer, Phys. Rev. **40**, 12079 (1989).
[14] E. Torfs, L. Stals, J. van Lunduyd, P. Delavignette, and S. Amelinckx, Phys. Status Solidi A **22**, 45 (1974).
[15] B. Roessler and J.A. Rayne, Phys. Rev. **136**, 1380A (1964).
[16] D.L. Martin, Phys. Rev. **17**, 1674 (1978).
[17] J.B. Staunton, B.L. Gyorffy, and P. Weinberger, J. Phys. F **10**, 2665 (1980).
[18] W.H. Fehlner and S.H. Vosko, Can. J. Phys. **54**, 2139 (1976).
[19] B. Ginatempo and J.B. Staunton, J. Phys. F **18**, 1827 (1988).
[20] J.S. Faulkner and G.M. Stocks, Phys. Rev. B **21**, 3222 (1980).
[21] H. Ebert, P. Weinberger, and J. Voitländer, Phys. Rev. B **31**, 7566 (1985).
[22] A. Gonis, G.M. Stocks, W.H. Butler, and H. Winter, Phys. Rev. B **29**, 555 (1984).
[23] J. Itoh, K. Asayama, and S. Kobayashi, Proc. Colloq. Ampere **13**, 162 (1964).
[24] G. Rienäcker and H. Gaubatz, Naturwissenschaften **28**, 534 (1940).
[25] M. Dixon and F.E. Hoare, Proc. Phys. Soc. London **90**, 253 (1967).
[26] D.L. Martin, Phys. Rev. **8**, 5357 (1973).
[27] P. Weinberger, J. Phys. F **12**, 2171 (1982).
[28] H. Eckardt, L. Fritsche, and J. Noffke, J. Phys. F **14**, 97 (1984).
[29] G.C. Carter, L.H. Bennett, and D.J. Kahan, *Metallic Shifts in NMR* (Pergamon, Oxford, 1977), Vol. 1.